J. Fluid Mech. (1980), *vol.* 97, *part* 1, *pp.* 145–155
Printed in Great Britain

Oseen velocity distributions in the wake of a flat plate

By TOSIO MIYAGI AND MICHIO NISHIOKA
College of Engineering, University of Osaka Prefecture, Sakai, Japan

(Received 19 June 1978 and in revised form 4 July 1979)

To account for our previous experimental results, the flow past a flat plate set parallel to a uniform stream is investigated on the basis of Oseen's equations of motion. We are mainly concerned with the wake region and calculate the velocity field in detail for the range of Reynolds numbers 20–3000, corresponding to the experiments. The calculation shows that there is a velocity overshoot in the velocity distribution near the trailing edge, with the same magnitude as in the experiments. Furthermore, we confirm the experimental fact that the velocity on the centre-line of wake recovers in proportion to the square root of the distance from the trailing edge in the near wake. The pressure field is also examined to see the streamwise pressure gradient in the near wake.

1. Introduction

One of the most interesting problems in the theory of viscous flow is the two-dimensional steady flow past a finite flat plate set parallel to a uniform stream. Goldstein (1930, 1933) investigated the development of the velocity distribution in the wake of the plate on the basis of boundary-layer theory. Recently, some attempts have also been made to solve the problem on the basis of the full Navier–Stokes equations of motion and higher-order boundary-layer theory (Talke & Berger 1970; Schneider & Denny 1971; Stewartson 1974; and others).

In a previous investigation (Nishioka & Miyagi 1978), we measured the velocity distributions in the completely laminar wakes at $R = 20$, 100, 400, 1200 and 3000, where R is the Reynolds number referred to the speed U_∞ of the uniform flow and the length l of the plate. One of the interesting findings from the experiments was the fact that in the near wake the velocity U_c on the centre-line recovers in proportion to the square root of the distance ξ from the trailing edge, i.e. $U_c \propto \xi^{\frac{1}{2}}$. So far as we know, the only theoretical result that seems to agree with this fact is Schneider & Denny's numerical solution for an extremely small region ($\xi < 0{\cdot}001$) enclosing the trailing edge, obtained on the basis of Navier–Stokes equations at $R = 10^5$, which is much higher than the Reynolds numbers of our experiments.

In the present paper we examine the velocity distributions in the wake on the basis of Oseen's equations of motion at $R = 20$ to 3000, and compare the solutions with our previous experiments. The present configuration, namely the parallel flat plate, is favourable to Oseen's approximation, because the normal velocity component will be very small everywhere. In addition, one may expect to obtain analytical results from Oseen equations, which are simpler than Navier–Stokes equations and yet retain the elliptic character of these equations. Therefore, Oseen equations may give

0022–1120/80/4392–8400 $02.00

us some qualitative results, if nonlinear effects do not play so crucial a role, though they may not be quantitatively correct. Here, with this expectation in mind, we endeavour to seek for some analytical results corresponding to our previous experiments.

2. Formulation and previous results

Suppose that an incompressible fluid of kinematic viscosity ν is in steady two-dimensional motion past a flat plate of length l set parallel to the uniform stream of speed U_∞. We take Cartesian co-ordinates (x, y) normalized by l, with the origin at the leading edge of the plate and the x axis along the direction of the stream, and we denote the x-, y- velocity components and the vorticity by $U_\infty(1+u)$, $U_\infty v$ and $U_\infty \omega/l = (U_\infty/l)(\partial v/\partial x - \partial u/\partial y)$, respectively. Then, Oseen's equation for the vorticity and the equation of continuity can be written as

$$(\Delta - R\partial/\partial x)\,\omega = 0, \quad R = U_\infty l/\nu, \tag{2.1}$$

$$\partial u/\partial x + \partial v/\partial y = 0, \tag{2.2}$$

where Δ stands for $\partial^2/\partial x^2 + \partial^2/\partial y^2$. The boundary conditions on the surface of the plate are

$$u = -1, \quad v = 0. \tag{2.3}$$

Bairstow, Cave & Lang (1923), and Oseen (1927) himself, reduced the problem given in the above differential form to an integral equation for the distribution function of fundamental singularities (the so-called Oseenlets) which are required to represent the plate. Later, the extension of this reformulation to the case of a cylinder of arbitrary cross-section was made by Miyagi (1964). Following his work, we may express the complex velocity $u - iv$ in the present case in terms of the distribution function $A(\tau)$ as:

$$u - iv = \int_0^1 [\tfrac{1}{2}R e^{\frac{1}{2}R\tilde{r}\cos\tilde{\theta}}\{K_0(\tfrac{1}{2}R\tilde{r}) + K_1(\tfrac{1}{2}R\tilde{r})\,e^{-i\tilde{\theta}}\} - e^{-i\tilde{\theta}}/\tilde{r}]\,A(\tau)\,d\tau, \tag{2.4}$$

where

$$\tilde{r} = [(x-\tau)^2 + y^2]^{\frac{1}{2}} \quad \text{and} \quad \tilde{\theta} = \tan^{-1}[y/(x-\tau)] \tag{2.5}$$

are polar co-ordinates whose origin is at the point τ on the plate where the typical Oseenlet is situated, and the K_n's are modified Bessel functions. It is noteworthy that $A(\tau)$ represents the shear force at τ on the plate. Letting the point (x, y) in (2.4) approach a point $(t_B, 0)$ on the body, we can apply the boundary conditions (2.3) and we then get the integral equation for $A(\tau)$, namely

$$\int_0^1 \kappa(t_B - \tau)\,A(\tau)\,d\tau = -1, \tag{2.6}$$

where the kernel is given by

$$\kappa(s) = \tfrac{1}{2}R e^{\frac{1}{2}Rs}[K_0(\tfrac{1}{2}R\,|s|) + \operatorname{sgn} s\, K_1(\tfrac{1}{2}R\,|s|)] - 1/s. \tag{2.7}$$

Once $A(\tau)$ is determined, the velocity field can be calculated from the equation (2.4). For large Reynolds numbers, $A(\tau)$ is given as

$$\begin{aligned} A(\tau) &= \sum_{k=1}^{4} A_k(\tau) + O(R^{-\frac{3}{2}}) \\ &= \underbrace{\frac{-1}{(\pi^3 R)^{\frac{1}{2}}}\frac{1}{\tau^{\frac{1}{2}}}}_{A_1(\tau)} - \underbrace{\frac{2}{\pi^3 R}\frac{\sin^{-1}\tau^{\frac{1}{2}}}{\tau(1-\tau)^{\frac{1}{2}}}}_{A_2(\tau)} + \underbrace{\frac{1}{(\pi^3 R)^{\frac{1}{2}}}\operatorname{erfc}[R(1-\tau)]^{\frac{1}{2}}}_{A_3(\tau)} - \underbrace{\frac{1}{\pi^2 R}\frac{e^{-R(1-\tau)}}{(1-\tau)^{\frac{1}{2}}}}_{A_4(\tau)} + O(R^{-\frac{3}{2}}), \end{aligned} \tag{2.8}$$

where erfc is the complementary error function defined as

$$\operatorname{erfc} z = \frac{2}{\pi^{\frac{1}{2}}} \int_z^\infty e^{-s^2}\, ds. \tag{2.9}$$

$A_1(\tau)$ and $A_2(\tau)$ were obtained by Piercy & Winny (1933). $A_3(\tau)$ and $A_4(\tau)$ were added by Seebass, Tamada & Miyagi (1966) to improve the solution by reconsidering the edge singularities.

3. The centre-line velocity U_c in the near wake

So far as we are concerned with the centre-line velocity, we may put $y = 0$ beforehand in the integrand of (2.4). Here, we focus our attention upon the near wake, where the distance ξ from the trailing edge is much smaller than unity. In fact, we assume that ξ is of order $R^{-\frac{1}{2}}$ and then $R\xi$ is of order $R^{\frac{1}{2}}$. Thus, the Bessel functions in (2.4) may be replaced by their asymptotic expansions, since their arguments are always positive and large. Then the centre-line velocity U_c may be written as

$$U_c = 1 + \sum_{k=1}^{4} (u_{k,1} + u_{k,2} + u_{k,3} + u_{k,4} + \ldots) + O(R^{-\frac{5}{4}}), \quad 1 \gg \xi \gg R^{-1}, \tag{3.1}$$

where

$$\left.\begin{aligned} u_{k,1} &= R(\tfrac{1}{2}\pi)^{\frac{1}{2}} \int_0^1 t^{-\frac{1}{2}} A_k(\tau)\, d\tau, \\ u_{k,2} &= -\tfrac{1}{2} R \int_0^1 t^{-1} A_k(\tau)\, d\tau, \\ u_{k,3} &= \tfrac{1}{8} R(\tfrac{1}{2}\pi)^{\frac{1}{2}} \int_0^1 t^{-\frac{3}{2}} A_k(\tau)\, d\tau, \\ u_{k,4} &= -\tfrac{3}{128} R(\tfrac{1}{2}\pi)^{\frac{1}{2}} \int_0^1 t^{-\frac{5}{2}} A_k(\tau)\, d\tau, \end{aligned}\right\} \tag{3.2}$$

and

$$t = \tfrac{1}{2} R(1 + \xi - \tau), \quad \xi = x - 1.$$

In what follows, we shall find approximate expressions for these integrals that are accurate to $O(R^{-1})$.

For the case $k = 1$, putting $\tau = (1+\xi)\cos^2\phi$, we can easily perform the integrations, obtaining

$$\left.\begin{aligned} u_{1,1} &= -1 + \frac{2}{\pi} \tan^{-1} \xi^{\frac{1}{2}} \doteqdot -1 + \frac{2}{\pi} \xi^{\frac{1}{2}} - \frac{2}{3\pi} \xi^{\frac{3}{2}} + O(R^{-\frac{5}{4}}), \\ u_{1,2} &= -\frac{1}{(\pi^3 R)^{\frac{1}{2}}} \frac{1}{(1+\xi)^{\frac{1}{2}}} \ln \frac{(1+\xi)^{\frac{1}{2}} - 1}{(1+\xi)^{\frac{1}{2}} + 1}, \\ u_{1,3} &= -\frac{1}{2\pi R} \frac{1}{1+\xi} \frac{1}{\xi^{\frac{1}{2}}} \doteqdot -\frac{1}{2\pi R} \frac{1}{\xi^{\frac{1}{2}}} + O(R^{-\frac{5}{4}}), \\ u_{1,4} &= O(R^{-\frac{5}{4}}). \end{aligned}\right\} \tag{3.3}$$

As will be seen below, $u_{1,2}$ exactly cancels with the first term of $u_{2,1}$.

For the case $k = 2$, integration is more difficult but can be carried out as follows. Putting $\tau = \sin^2\phi$ and integrating by parts, we have

$$u_{2,1} = \frac{2}{(\pi^5 R)^{\frac{1}{2}}} \frac{1}{(1+\xi)^{\frac{1}{2}}} \left[I_1(\xi) + \int_0^{\frac{1}{2}\pi} \ln \frac{1-\cos\phi}{1+\cos\phi} d\phi \right], \tag{3.4}$$

where

$$\left.\begin{aligned} I_1(\xi) &= \int_0^{\frac{1}{2}\pi} \ln \frac{(1+\xi)^{\frac{1}{2}}(\xi+\cos^2\phi)^{\frac{1}{2}} + \xi - \cos\phi}{(1+\xi)^{\frac{1}{2}}(\xi+\cos^2\phi)^{\frac{1}{2}} + \xi + \cos\phi} d\phi, \\ \int_0^{\frac{1}{2}\pi} \ln \frac{1-\cos\phi}{1+\cos\phi} d\phi &= -4G, \end{aligned}\right\} \tag{3.5}$$

and G is Catalan's constant† $\left(G = \sum_{m=0}^{\infty} (-1)^m/(2m+1)^2 = 0{\cdot}91596\ldots\right)$. To evaluate $I_1(\xi)$, we may differentiate (3.5) with respect to ξ and then integrate it. Thus, we have

$$\frac{dI_1}{d\xi} = \frac{1}{\xi(1+\xi)^{\frac{1}{2}}} \left(\frac{\pi}{2} - \tan^{-1}\xi^{\frac{1}{2}} \right). \tag{3.6}$$

By considering the behaviour of $I_1(\xi)$ for $\xi \ll 1$, the integration of (3.6) gives

$$I_1(\xi) = 4G + \tfrac{1}{2}\pi \ln \frac{(1+\xi)^{\frac{1}{2}} - 1}{(1+\xi)^{\frac{1}{2}} + 1} - \int_0^{\xi} \frac{\tan^{-1}\delta^{\frac{1}{2}}}{\delta(1+\delta)^{\frac{1}{2}}} d\delta. \tag{3.7}$$

Thus, we arrive at

$$\begin{aligned} u_{2,1} &= \frac{1}{(\pi^3 R)^{\frac{1}{2}}} \frac{1}{(1+\xi)^{\frac{1}{2}}} \ln \frac{(1+\xi)^{\frac{1}{2}} - 1}{(1+\xi)^{\frac{1}{2}} + 1} - \frac{2}{(\pi^5 R)^{\frac{1}{2}}} \frac{1}{(1+\xi)^{\frac{1}{2}}} \int_0^{\xi} \frac{\tan^{-1}\delta^{\frac{1}{2}}}{\delta(1+\delta)^{\frac{1}{2}}} d\delta \\ &\fallingdotseq \frac{1}{(\pi^3 R)^{\frac{1}{2}}} \frac{1}{(1+\xi)^{\frac{1}{2}}} \ln \frac{(1+\xi)^{\frac{1}{2}} - 1}{(1+\xi)^{\frac{1}{2}} + 1} - \frac{4}{(\pi^5 R)^{\frac{1}{2}}} \xi^{\frac{1}{2}} + O(R^{-\frac{5}{4}}). \end{aligned} \tag{3.8}$$

By a similar argument $u_{2,2}$ becomes

$$\begin{aligned} u_{2,2} &= \frac{1}{\pi^3 R} \frac{1}{1+\xi} \left[\frac{\pi^2}{\xi^{\frac{1}{2}}} + \frac{1}{\xi^{\frac{1}{2}}} \int^{\xi} \frac{1}{\delta^{\frac{1}{2}}(1+\delta)^{\frac{1}{2}}} \ln \frac{(1+\delta)^{\frac{1}{2}} - 1}{(1+\delta)^{\frac{1}{2}} + 1} d\delta + 8G \right] \\ &\fallingdotseq \frac{1}{\pi R} \frac{1}{\xi^{\frac{1}{2}}} + \frac{2}{\pi^3 R} \left(\ln \frac{\xi}{4} + 4G - 2 \right) + O(R^{-\frac{5}{4}}). \end{aligned} \tag{3.9}$$

We can calculate $u_{2,3}$ by the same procedure; the result is

$$u_{2,3} = -\frac{1}{2} \frac{1}{(\pi^3 R^3)^{\frac{1}{2}}} \frac{1}{\xi} + O(R^{-\frac{3}{2}}). \tag{3.10}$$

We now proceed to the case $k = 3$. After the transformation $[R(1-\tau)]^{\frac{1}{2}} = \delta$, integration by parts gives

$$\begin{aligned} u_{3,1} &= \frac{2\xi^{\frac{1}{2}}}{\pi} \left[-1 + \frac{2}{\pi^{\frac{1}{2}}} \int_0^{R^{\frac{1}{4}}} \left(1 + \frac{\delta^2}{R\xi} \right)^{\frac{1}{2}} e^{-\delta^2} d\delta \right] \\ &\fallingdotseq \frac{1}{2\pi R} \frac{1}{\xi^{\frac{1}{2}}} + O(R^{-\frac{5}{4}}). \end{aligned} \tag{3.11}$$

† See, for example, I. S. Gradshteyn & I. M. Ryzhik, *Table of Integrals, Series and Products* p. 529 (Academic, 1965).

under the assumption that $R\xi = O(R^{\frac{1}{2}})$. The following expressions are obtained in a similar manner:

$$\left.\begin{aligned} u_{3,2} &= -\frac{1}{2}\frac{1}{(\pi^3R^3)^{\frac{1}{2}}}\frac{1}{\xi}+O(R^{-\frac{3}{2}}),\\ u_{3,3} &= O(R^{-\frac{5}{4}}),\\ u_{4,1} &= -\frac{1}{\pi R}\frac{1}{\xi^{\frac{1}{2}}}+O(R^{-\frac{5}{4}}),\\ u_{4,2} &= \frac{1}{(\pi^3R^3)^{\frac{1}{2}}}\frac{1}{\xi}+O(R^{-\frac{3}{2}}),\\ u_{4,3} &= O(R^{-\frac{5}{4}}). \end{aligned}\right\} \tag{3.12}$$

Gathering above results together, we find the analytical expression for U_c in the form:†

$$U_c = \frac{2}{\pi}\xi^{\frac{1}{2}} - \left\{\frac{2}{3\pi}\xi + \frac{4}{(\pi^5R)^{\frac{1}{2}}}\right\}\xi^{\frac{1}{2}} + \frac{2}{\pi^3R}(\ln\tfrac{1}{4}\xi + 4G - 2) + O(R^{-\frac{5}{4}}). \tag{3.13}$$

It should be noted that the first, second and third terms are of orders $R^{-\frac{1}{4}}$, $R^{-\frac{3}{4}}$ and R^{-1} respectively, and the dominant term does not depend on the Reynolds number and is proportional to $\xi^{\frac{1}{2}}$. It will be also of interest that the first term of (3.13) originates from the singularity at the leading edge.

In figure 1, the values of U_c calculated for $R = 3000$ are represented by thick full line and they are compared with our experimental data and other theoretical and experimental results. They agree satisfactorily and confirm the experimental findings that $U_c \propto \xi^{\frac{1}{2}}$ for $\xi < 0{\cdot}5$. The thin full line for $R = 3000$ and the broken line for $R = 20$ were obtained in the manner described in the next section. It may be added that the curves for $R = 100$, 400 and 1200 obtained from (3.13) lie between the curves for $R = 20$ and 3000, though they are not shown here.

4. The velocity distribution in the wake

Since (2.8) is not accurate to estimate the velocity field for smaller Reynolds numbers (for example, $R = 20$), we must adopt the method of numerical computations to determine $A(\tau)$. Such a numerical method has already been developed for the cases of a normal flat plate and a circular cylinder by Miyagi (1968, 1974).

We divide the interval of the integral (2.6) into n equal parts. Thus, we have

$$\sum_{p=1}^{n}\int_{(p-1)/n}^{p/n}\kappa(t_B-\tau)\,a_p(\tau)\,d\tau = -1, \tag{4.1}$$

where $a_p(\tau)$ denotes unknown distribution function in the pth sub-interval. When n is large, each sub-interval of the integral becomes very small so that within the pth sub-interval $a_p(\tau)$ may be assumed to be constant and equal to a_p, say. Further, it is convenient to set marked point t_B at the middle point of each interval in turn. Then,

† During the present work, we became aware of the fact that equation (12) in the paper by Seebass *et al.* (1966) gives the Fourier transform of the perturbation velocity as $\hat{h}_-(p)$. So, following the method of these authors, we can obtain an approximate expression for the velocity on the centre-line, namely

$$U_c = 1 - e^{\xi/2\pi}\operatorname{erfc}(\xi/2\pi)^{\frac{1}{2}}$$

although they did not give this expression. For $\xi \ll 1$, this leads to $U_c = (\sqrt{(2)}/\pi)\xi^{\frac{1}{2}} + \ldots$.

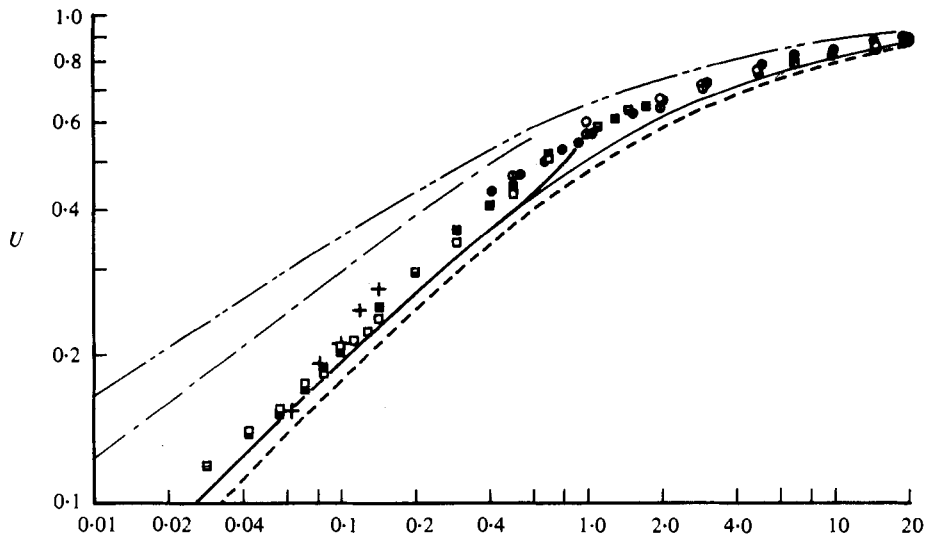

FIGURE 1. Non-dimensional velocity on centre-line of wake U_c *vs.* non-dimensional distance from trailing edge ξ. Present calculations: ——, analytical result for $R = 3000$ [equation (3.13)]; ——, numerical result for $R = 3000$; – – –, numerical result for $R = 20$. Other theoretical results: — – —, Schneider & Denny (1971), $R = 10^5$; — – – —, Goldstein (1933). Measurements of Nishioka & Miyagi (1978): ○, $R = 20$; ⓘ, $R = 100$; ●, $R = 400$; □, $R = 1200$; ■, $R = 3000$. Measurement of Mattingly & Criminale (1972): +, $R \doteqdot 10^4$.

by considering each of the n positions for t_B, we obtain n linear algebraic equations for the unknowns a_p ($p = 1, 2, \ldots, n$).

As can be seen from the structure of the analytical solution (2.8), the exact distribution function should have singularities at the points $\tau = 0$ and 1. So we take into account these singularities in such a way that $a_1(\tau) = a_1'/\tau^{\frac{1}{2}}$ and $a_n(\tau) = a_n'/(1-\tau)^{\frac{1}{2}}$, where a_1' and a_n' are unknown constants. Thus, we can estimate numerically the distribution functions for any Reynolds number. To convince ourselves of the accuracy of this numerical procedure, we computed the distribution functions for $R = 100$, 400, 1200 and 3000, and we confirmed good agreements with the corresponding analytical solutions.

To determine the velocity field, we have integrated (2.4) numerically using the distribution function obtained by the above method with $n = 16$ for the case $R = 20$ and the analytical result (2.8) for the case $R = 3000$.

The computed velocity distribution in the near wake at $R = 3000$ is shown in figure 2, together with the previous experimental data. The experiment indicates that the velocity distribution at the trailing edge is almost of the Blasius type except for the presence of the velocity overshoot in the outer parts. The subsequent deviation of the distribution from the Blasius occurs only in the inner part, that is, the outer part remains almost unchanged even up to $\xi = 0{\cdot}15$. It may be seen from figure 2 that these features are well predicted by the present results, although the calculated wake is thinner than the observed one.

In figure 3, the velocity distributions in the far wake for $R = 20$ and 3000 are also compared with the corresponding experimental data. The agreement between the

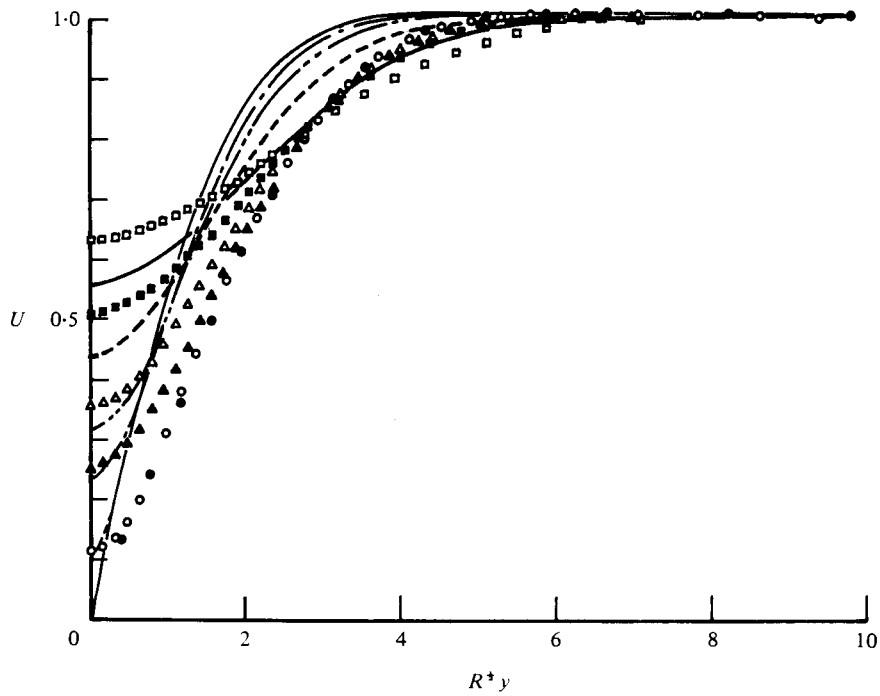

FIGURE 2. Velocity distributions in the near wake at $R = 3000$. Present calculations (lines) are compared with measurements of Nishioka & Miyagi (1971) (symbols). ——, ●, $\xi = 0$; – – –, ○, $\xi = 0{\cdot}0285$; — – —, ▲, $\xi = 0{\cdot}15$; — – – —, △, $\xi = 0{\cdot}30$; – – –, ■, $= 0{\cdot}70$; ——, □, $\xi = 1{\cdot}5$.

theory and experiment is satisfactory in the far wake, as the comparison at $\xi = 5$ shows. At stations $\xi = 0$ to 1·0, the non-dimensional half-width of the wake is thinner at $R = 20$ than at $R = 3000$ in the experiments. This is also the case in the present theory. Moreover, the present theory predicts a velocity overshoot of the same magnitude as that observed in the experiments.

5. The pressure field

For small Reynolds numbers, it is well known that the pressures at the edges of the plate have singularities of the Stokes type, $(r e^{i\theta})^{-\frac{1}{2}}$, where (r, θ) are polar co-ordinates referred to the point under discussion. For large Reynolds numbers, however, it is not self-evident whether the pressures in the vicinity of edges still have these singularities. In Oseen flows the pressure p is harmonic and is given by

$$p = \int_0^1 \frac{\cos\tilde{\theta}}{\tilde{r}} A(\tau)\, d\tau. \tag{5.1}$$

Hence we can easily evaluate the contribution of $A_1(\tau)$ in (2.8) to the pressure p_L at the leading edge as

$$p_L = \frac{1}{(\pi R)^{\frac{1}{2}}} \frac{\sin\frac{1}{2}\theta_L}{r_L^{\frac{1}{2}}} + \ldots, \quad 1 \gg R r_L > 0, \tag{5.2}$$

where (r_L, θ_L) are polar co-ordinates referred to the leading edge.

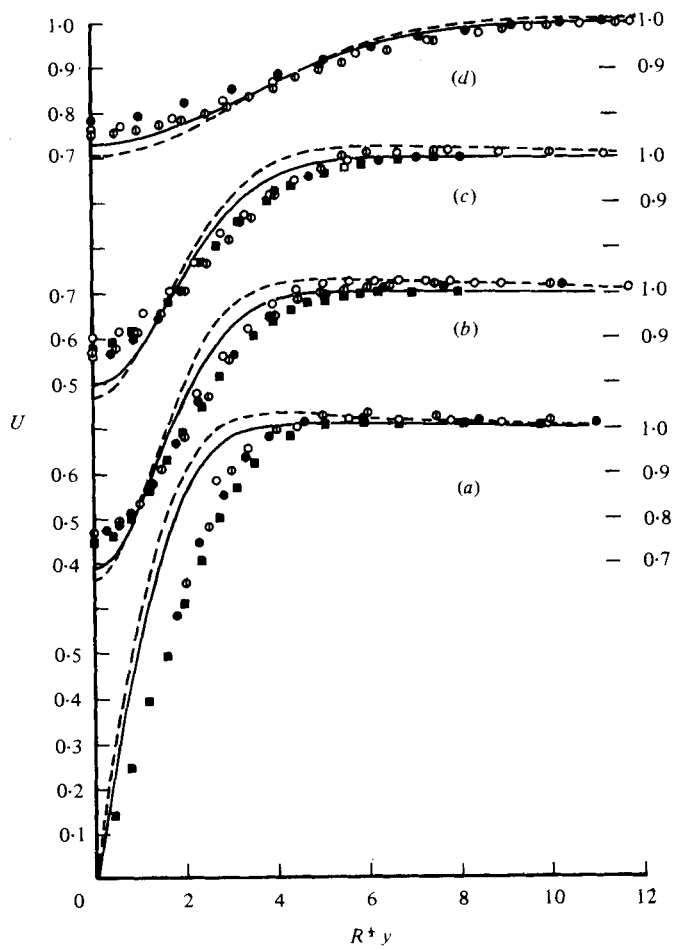

FIGURE 3. Wake development at $R = 20$ to 3000.

		Present		Measurements of Nishioka & Miyagi (1978)			
		– – –	———	○	⊖	●	■
R		20	3000	20	100	400	3000
ξ	(*a*)	0	0	0	0	0	0
	(*b*)	0·5	0·5	0·5	0·5	0·54	0·5
	(*c*)	1·0	1·0	1·0	1·0	1·05	1·10
	(*d*)	5·0	5·0	5·0	5·0	5·15	—

At the trailing edge, on the other hand, its contribution p_1 becomes logarithmic and is not Stokes type, i.e.

$$p_1 = \frac{1}{(\pi^3 R)^{\frac{1}{2}}} \ln \tfrac{1}{4} r_T + \ldots, \quad 1 \gg R r_T > 0, \tag{5.3}$$

where we have taken polar co-ordinates (r_T, θ_T) referred to the trailing edge. In this connexion, it should be remembered that the first term $A_1(\tau)$ is singular at the leading edge only.

The calculation of the contribution p_2 from the second term $A_2(\tau)$ is somewhat cumbersome, but it proceeds as follows: putting $\tau = \sin^2\phi$ and integrating by parts, we have

$$\left.\begin{aligned} p_2 &= -\frac{4}{\pi^3 R}\left[\phi I_2(\phi)\Big|_0^{\frac{1}{2}\pi} - \int_0^{\frac{1}{2}\pi} I_2(\phi)\,d\phi\right], \\ \text{where} \qquad I_2(\phi) &= \int \frac{x-\sin^2\phi}{(x-\sin^2\phi)^2+y^2}\frac{d\phi}{\sin\phi}. \end{aligned}\right\} \tag{5.4}$$

Further, through the substitution $\cos\phi = \delta$, and a decomposition into partial fractions, we get

$$\begin{aligned} p_2\Big/\left(\frac{4}{\pi^3 R}\right) = {} & \frac{x}{2(x^2+y^2)}\int_0^{\frac{1}{2}\pi} \ln\frac{1-\cos\phi}{1+\cos\phi}\,d\phi \\ & + \frac{cf-d}{8fB(x^2+y^2)}\int_0^{\frac{1}{2}\pi} \ln\frac{\cos^2\phi+2B\cos\phi+f}{\cos^2\phi-2B\cos\phi+f}\,d\phi \\ & - \frac{cf+d}{4fA(x^2+y^2)}\int_0^{\frac{1}{2}\pi}\left(\tan^{-1}\frac{\cos\phi+B}{A}+\tan^{-1}\frac{\cos\phi-B}{A}\right)d\phi, \end{aligned} \tag{5.5}$$

where

$$\begin{gathered} c = x, \quad d = x^2-x-y^2, \quad f = [(x-1)^2+y^2]^{\frac{1}{2}}, \quad g = x-1, \\ A = [\tfrac{1}{2}(f+g)]^{\frac{1}{2}}, \quad B = [\tfrac{1}{2}(f-g)]^{\frac{1}{2}}. \end{gathered} \tag{5.6}$$

The first integral is equal to $-4G$, as seen in the above. Differentiating the second integral, I_3, in (5.5) with respect to r_T and introducing the substitution $\tan\frac{1}{2}\phi = \delta$ produces an integral which can be integrated to give

$$\frac{\partial I_3}{\partial r_T} = -\frac{\sin\frac{1}{2}\theta_T}{r_T^{\frac{1}{2}}}\ln\tfrac{1}{4}r_T - \theta_T\frac{\cos\frac{1}{2}\theta_T}{r_T^{\frac{1}{2}}} + \ldots, \quad 1 \gg Rr_T > 0. \tag{5.7}$$

It immediately follows that

$$I_3 = -2r_T^{\frac{1}{2}}[\{\ln\tfrac{1}{4}r_T - 2\}\sin\tfrac{1}{2}\theta_T + \theta_T\cos\tfrac{1}{2}\theta_T] + \ldots, \quad 1 \gg Rr_T > 0. \tag{5.8}$$

The third integral I_4 is given in a like manner by

$$I_4 = \frac{\pi^2}{2} + r_T^{\frac{1}{2}}[\{\ln\tfrac{1}{4}r_T - 2\}\cos\tfrac{1}{2}\theta_T - \theta_T\sin\tfrac{1}{2}\theta_T] + \ldots, \quad 1 \gg Rr_T > 0. \tag{5.9}$$

From these results, we obtain the expression for the pressure p_2 in an extremely small region including the trailing edge as

$$p_2 = -\frac{1}{\pi R}\frac{\cos\frac{1}{2}\theta_T}{r_T^{\frac{1}{2}}} - \frac{2}{\pi^3 R}[\ln\tfrac{1}{4}r_T + 4G - 2] + \ldots, \quad 1 \gg Rr_T > 0. \tag{5.10}$$

The contributions p_3 and p_4 of $A_3(\tau)$ and $A_4(\tau)$ respectively, are also given as

$$p_3 = -\frac{1}{(\pi^3 R)^{\frac{1}{2}}}[\ln(4Rr_T) + \gamma] + \ldots, \quad 1 \gg Rr_T > 0, \tag{5.11}$$

$$p_4 = -\frac{1}{\pi R}\frac{\cos\frac{1}{2}\theta_T}{r_T^{\frac{1}{2}}} + \frac{2}{(\pi^3 R)^{\frac{1}{2}}} + \ldots, \quad 1 \gg Rr_T > 0, \tag{5.12}$$

by making use of the transformation of these integrals into the type of Laplace's integral transform ($\gamma = 0{\cdot}5772\ldots$).

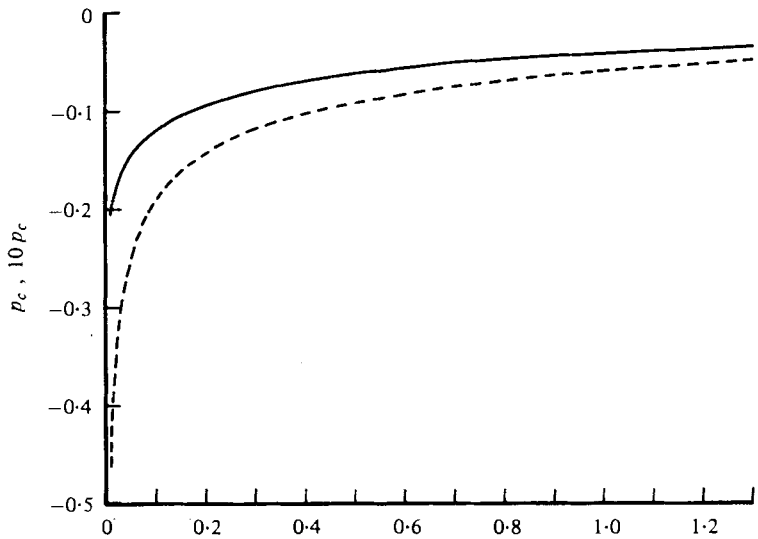

FIGURE 4. Non-dimensional pressure on centre-line of wake p_c *vs.* non-dimensional distance from trailing edge ξ. Plotted are p_c for $R = 20$ (– – – –) and $10p_c$ for $R = 3000$ (——).

Thus, final results $\sum_{k=1}^{4} p_k$ show that the pressure singularity is of Stokes type there also for high Reynolds numbers, though the factor R^{-1} is different from the factor $R^{-\frac{1}{2}}$ in the corresponding expression at the leading edge.

In the course of the calculation of the velocity field, we have already evaluated the integral (5.1), that is, the pressure given by (5.1) is equal to the real part of the harmonic part of the perturbation velocity. In figure 4, the pressure on the wake centre-line, p_c (the pressure coefficient referred to the dynamic pressure of the uniform flow), is plotted against ξ for $R = 20$ and 3000, and this graph indicates the importance of the streamwise pressure gradient. The appearance of the velocity overshoot may be due to this strong suction at the trailing edge, though the suction may be finite in experiments.

This suction affects the flow approaching the trailing edge. Indeed, the velocity overshoot appears even upstream of the trailing edge, as was found in our previous experiments. This elliptic character of the flow cannot be described by the boundary-layer theory. Furthermore, the streamwise pressure gradient is considerable in the near wake, as shown in figure 4. These may be the main reasons for the disagreements between our experimental results and those of Goldstein (1930), who used the boundary-layer approximation and assumed the wake to be isobaric. We expect that a more complete solution of Navier–Stokes equation may settle this problem.

REFERENCES

BAIRSTOW, L., CAVE, B. M. & LANG, E. D. 1923 *Phil. Trans. Roy. Soc.* A **223**, 383.
GOLDSTEIN, S. 1930 *Proc. Camb. Phil. Soc.* **26**, 1.
GOLDSTEIN, S. 1933 *Proc. Roy. Soc.* A **142**, 546.
MATTINGLY, G. E. & CRIMINALE, W. O. 1972 *J. Fluid Mech.* **51**, 233.
MIYAGI, T. 1964 *J. Phys. Soc. Japan* **19**, 1063.
MIYAGI, T. 1968 *J. Phys. Soc. Japan* **24**, 204.
MIYAGI, T. 1974 *J. Phys. Soc. Japan* **37**, 1699.
NISHIOKA, M. & MIYAGI, T. 1978 *J. Fluid Mech.* **84**, 705.
OSEEN, C. W. 1927 *Hydrodynamik*. Leipzig: Akademische.
PIERCY, N. A. V. & WINNY, H. F. 1933 *Proc. Roy. Soc.* A **140**, 543.
SCHNEIDER, L. I. & DENNY, V. E. 1971 *A.I.A.A. J.* **9**, 655.
SEEBASS, R., TAMADA, K. & MIYAGI, T. 1966 *Phys. Fluids* **9**, 1697.
STEWARTSON, K. 1974 *Adv. Appl. Mech.* **14**, 145.
TALKE, F. E. & BERGER, S. A. 1970 *J. Fluid Mech.* **40**, 161.